ELSEVIER

Ceramics International 31 (2005) 757–763

CERAMICS INTERNATIONAL

www.elsevier.com/locate/ceramint

Densification behaviour of a red firing Brazilian kaolinitic clay

F.A.C. Milheiro, M.N. Freire, A.G.P. Silva, J.N.F. Holanda*

Northern Fluminense State University, Advanced Materials Laboratory, Campos dos Goytacazes, RJ 28013-602, Brazil

Received 13 January 2004; received in revised form 1 July 2004; accepted 22 August 2004
Available online 13 December 2004

Abstract

This study focuses on the complexity of the densification of a Brazilian kaolinitic clay sintered in air at various temperatures. The used kaolinitic clay comes from a large structural ceramics production region in South-Eastern Brazil (Campos-RJ). The samples were dry pressed in a cylindrical die and sintered at temperatures ranging from 750 °C to 1150 °C. XRD and SEM were used to identify the present phases and the densification level. The densification was measured by five parameters: specific surface, linear shrinkage, water absorption, apparent density, and compressive strength. The results revealed that sintering is governed by different mechanisms according to the temperature. A series of phase transformations takes place during sintering, which play an important role on the densification. Below 950 °C, sintering is governed by solid state diffusion mechanisms. Above 950 °C, sintering is governed by viscous flow mechanism with high influence on the densification of the green body. In addition, the red clay presented a refractory behaviour during firing due the high amount of kaolinite clay mineral, high loss on ignition, and the presence of gibbsite, which impairs sintering, resulting in greater porosity of the specimens.

Keywords: A. Firing; B. Microstructure-final; D. Clays; E. Structural applications

1. Introduction

It is well-known that kaolinite is one of the most widely used clay minerals, being a major component of the raw materials used in the manufacture of pottery, cement, and structural clay products. Kaolinite is a two layer 1:1 silicate, $Al_2O_3{\cdot}2SiO_2{\cdot}2H_2O$, and is the principal specimen of its group [1]. It is structurally formed by one layer of tetrahedral silica (SiO_4), and one layer of octahedral gibbsite ($Al_2O_3{\cdot}3H_2O$), neither bearing cations nor H_2O molecules between the structural layers. The kaolinite crystal consists of about 40–50 structural two-layers units held together by hydrogen bonds, which act between the OH groups of the gibbsite layer of one unit and the oxygen atoms of the silica layer of an adjacent unit. This type of clay mineral is generally found in acidic tropical soils in areas with high rainfall. However, the mined kaolinite is generally associated with the presence of various impurities depending on the geological conditions under which the kaolinite was formed [2]. These impurities can modify the physical and chemical properties of a kaolinite and affect its use as an industrial mineral.

In South-Eastern Brazil (Campos-RJ), there are extensive quaternary sedimentary clay deposits mainly localized on the right riverside of the Paraíba do Sul river. Clays from this region are rich in kaolinite [3,4] and widely used as raw materials for red bricks and roofing tiles by the local ceramic industry, which assembles about 110 plants. However, the quality of these ceramic products is often poor, in particular there is the lack of more knowledge on the densification of these kaolinitic clays. In addition, these clays are also being submitted to testing in ceramic tiles. Thus, the densification behaviour of kaolinitic clays from Campos-RJ during the sintering step is still to be investigated and has both academic value and immediate commercial importance.

In this study, an effort has been made to describe the densification behaviour of a representative natural red clay sample from South-Eastern Brazil (Campos-RJ) as a function of the sintering temperature. Emphasis is given to the clay characteristics and phase and microstructural

* Corresponding author. Tel.: +55 222 726 1623; fax: +55 222 726 1533.
E-mail address: holanda@uenf.br (J.N.F. Holanda).

0272-8842/$30.00
doi:10.1016/j.ceramint.2004.08.010

changes of the pressed specimens taking place during the sintering step.

2. Experimental procedures

The kaolinitic clay powder sample was collected from a deposit located in South-Eastern Brazil (Campos-RJ). This deposit is representative and widely used by ceramic plants. The sample was dried and sieved to pass a 60 mesh sieve. Particle size data of the sample are summarized in Table 1.

Chemical analysis of the clay powder was determined by atomic emission spectrophotometry with inductively coupled plasma (ICP-AES Instrument, ARL-3410). X-ray diffraction analysis was performed (URD-65 Diffractometer, Seifert) using monochromatic Cu Kα radiation at 40 kV and 40 mA over non-oriented specimen. Scanning speed was 1.5° (2θ)/min. The phases were identified from peak positions and intensities using reference data from the JCPDS handbook [5]. TGA/DTG/DTA were carried out on the as-received sample (SDT-2960 Simultaneous TGA-DTA, TA Instruments) under air atmosphere from room temperature up to 1150 °C at a heating rate of 10 °C/min.

Cylindrical ceramic pellets (ϕ = 10 mm) were obtained by uniaxial pressing at 25 MPa. After pressing, the green bodies were dried for 24 h at 110 °C. The sintering step was carried out at soaking temperatures varying from 750 °C to 1150 °C for 1 h. The heating rate up to 600 °C was 2 °C/min, followed by a 1 h hold at 600 °C, and 10 °C/min up to maximum temperature.

The densification behaviour was described in terms of specific surface, linear shrinkage, water absorption, apparent density, and diametral compressive strength. Linear shrinkage values upon drying and sintering were evaluated from the variation of the length of the cylindrical bodies. Water absorption values were determined from the weight differences between the as-sintered and the water saturated samples (immersed for 2 h in boiling water). The apparent density values were determined by the Archimedes method of immersion in water. The diametral compressive strength values [6,7] were determined by using an universal testing machine (model 5582, Instron). The crossbar speed was hold at 0.5 mm/min for all tests. In addition, the specific surface area of the specimens was measured in an Autosorb-1 equipment (model ASIC-VPL, Quantachrome Instruments) by nitrogen adsorption according the BET method.

The phases identification of the sintered specimens was performed by X-ray diffraction. The sintered microstructure was observed by scanning electron microscopy (DSM 962, Zeiss).

Table 1
Particle size distribution for the studied clay (wt.%)

Clay (<2 μm)	Silt (2 ≤ x < 60 μm)	Sand (60 ≤ x < 600 μm)
56	37	7

Table 2
Chemical composition (wt.%) for studied clay

SiO_2	42.09
Al_2O_3	30.90
Fe_2O_3	10.92
CaO	0.13
MgO	0.74
MnO	0.03
TiO_2	1.28
Na_2O	0.32
K_2O	1.04
Loss on ignition	12.55

3. Results and discussion

During heating two kinds of processes take place: decomposition—phase transformations and sintering. The decomposition and phase transformations influence the evolution and intensity of the sintering process.

Chemical composition and the loss on ignition of the clay powder is shown in Table 2. The clay powder is constituted mainly by SiO_2 and Al_2O_3, which correspond to about 73%. The high loss on ignition (12.55%) is associated with the presence of clay minerals, hydroxides, and organic matter. The amount of Alkaline oxides (K_2O and Na_2O) is low. The amount of earth-alkaline oxides (CaO and MgO) also is low, and indicate that the studied red clay is poor in carbonates. The chemical analysis of the clay powder also showed a large amount of Fe_2O_3 (10.92 %). This oxide gives the reddish color of the clay-based products after sintering. This oxide is present in form of goethite. Additionally, Fe^{3+} cations can partially substitute the Al^{3+} cations in the octahedral sites of the kaolinite structure [8].

Fig. 1 shows the X-ray diffraction pattern of the clay powder. The following mineralogical phases were identified: kaolinite ($Al_2O_3{\cdot}2SiO_2{\cdot}2H_2O$), gibbsite ($Al_2(OH)_6$), illite/mica and quartz (SiO_2). Goethite also has been identified by its weaker diffraction lines. Rational mineralogical composition analysis [1,9] showed that it contained: kaolinite (73.2%), illite/mica (8.2%), gibbsite (6.5%) and quartz (12.1%). Due to the large amount of kaolinite throughout this paper the clay is referred to as red kaolinitic clay.

Fig. 2 shows the diffraction patterns of the clay specimens after firing for 1 h between 750 °C and 1150 °C. Based on the X-ray diffraction patterns and previous studies [10–13] it is possible to describe the transformations underwent by the clay at different temperatures. At 750 °C, the peaks of kaolinite and gibbsite are not seen. Kaolinite is transformed into metakaolinite. Gibbsite has likely been transformed into a transition alumina phase [14]. The peaks of quartz and illite/mica are still seen. Peaks of δ-Al_2O_3 are identified at 850 °C and 900 °C. At 950 °C peaks of γ-Al_2O_3, spinel and mullite appear. The latter phases are developed from the metakaolinite by topotactical reactions. Above 1000 °C cristobalite is beginning to develop. At 1150 °C the peaks of illite/mica are not seen but those of γ-Al_2O_3, spinel and mullite remain.

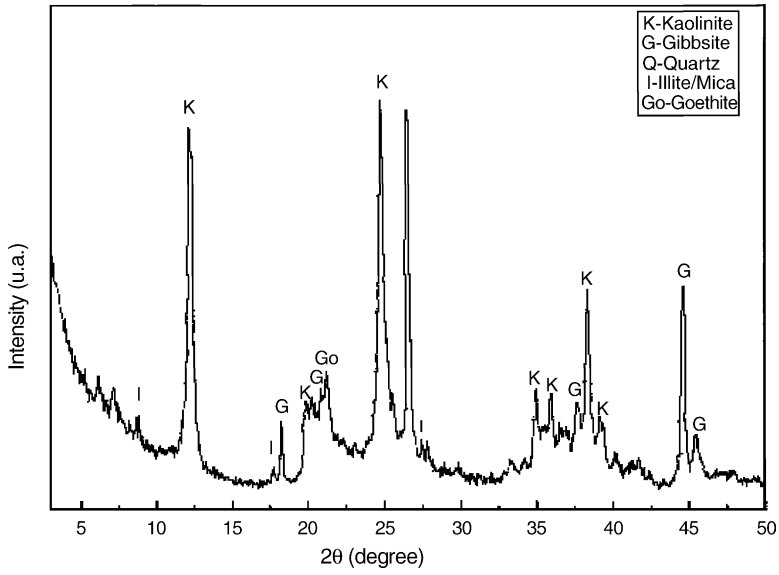

Fig. 1. X-ray diffraction pattern for the kaolinitic clay powder.

The TG/DTG/DTA curves are shown in Fig. 3. Three weight loss events are seen in the TG and DTG curves at 60.02 °C, 271.40 °C and 499.34 °C. The first endothermic event concerns to the evolution of the physically adsorbed water by the kaolinite. The second weight loss occurs due to the evolution of water resulting from the dehydration of gibbsite and its subsequent transformation into a transition alumina phase. The third weight loss is again caused by water evolution, but due to the dehydroxylation of kaolinite, which transforms into metakaolinite. The loss of the OH groups of the octahedral layer (the gibbsite layer) distorts the atomic order of this layer but the tetrahedral layer (silica layer) is less affected. The SiO_4 tetrahedra hold their form and a limited order is supposed to exist in the (1 1 0) plane [15]. The metakaolinite particles hold the platelet shape of the kaolinite. The final weight loss totals 15.13% against 13.95% of the weight loss of pure kaolinite. There is a small exothermic peak at 958.97 °C. It is likely related to the formation of a Si-containing γ-Al_2O_3 with spinel structure and/or primary mullite [16–18]. Spinel γ-Al_2O_3 and mullite are formed from the reaction between the constituents of metakaolinite. Amorphous silica is also formed [17]. Fig. 4 outlines the events occurring during heating at their respective temperatures and describes the possible reactions [1,11,16,18].

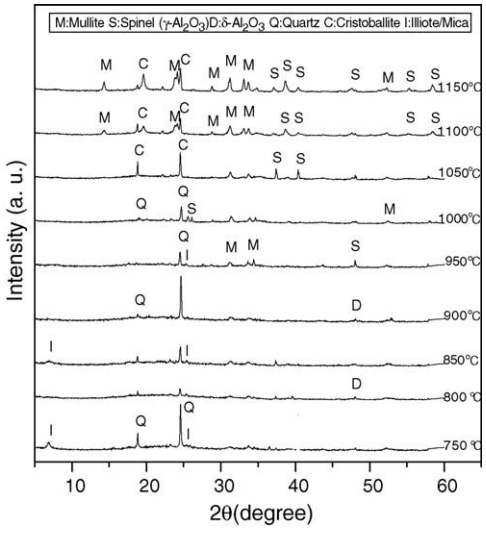

Fig. 2. X-ray diffraction patterns for the kaolinitic clay sintered at various temperatures.

In order to enlighten the densification behaviour on sintering, the fracture surface of the as-fired samples were examined (see Fig. 5a–d). The micrographs show the evolution of the structure of the kaolinitic clay as temperature increases. At 750 °C (Fig. 5a) the surface is rough and the porosity is clearly visible. The metakaolinite can be seen. At 950 °C (Fig. 5b), a finer morphology is found, showing well-bonded aggregates rather than detached particles. Above 950 °C the porosity starts to reduce (Fig. 5c). At 1150 °C (Fig. 5d), the structure is totally dense. In this case, the elimination of a large amount of open porosity that exists within the structure occurred. The evolution of the specific surface area is shown in Fig. 6. A reduction of the specific surface area is observed as temperature increases. This behaviour agrees with the observation of the structures. The specific surface area of the kaolinitic clay increases after its decomposition. The process of dehydroxylation of the kaolinite from the octahedral layer creates cracks and pores on the surface of the platelets. The high specific surface area works as the driving force for sintering. It decreases almost linearly with the temperature increase.

Fig. 7 shows the linear shrinkage of the sintered specimens. It is noticed that the linear shrinkage behaves differently below and above 950 °C. This is related to the

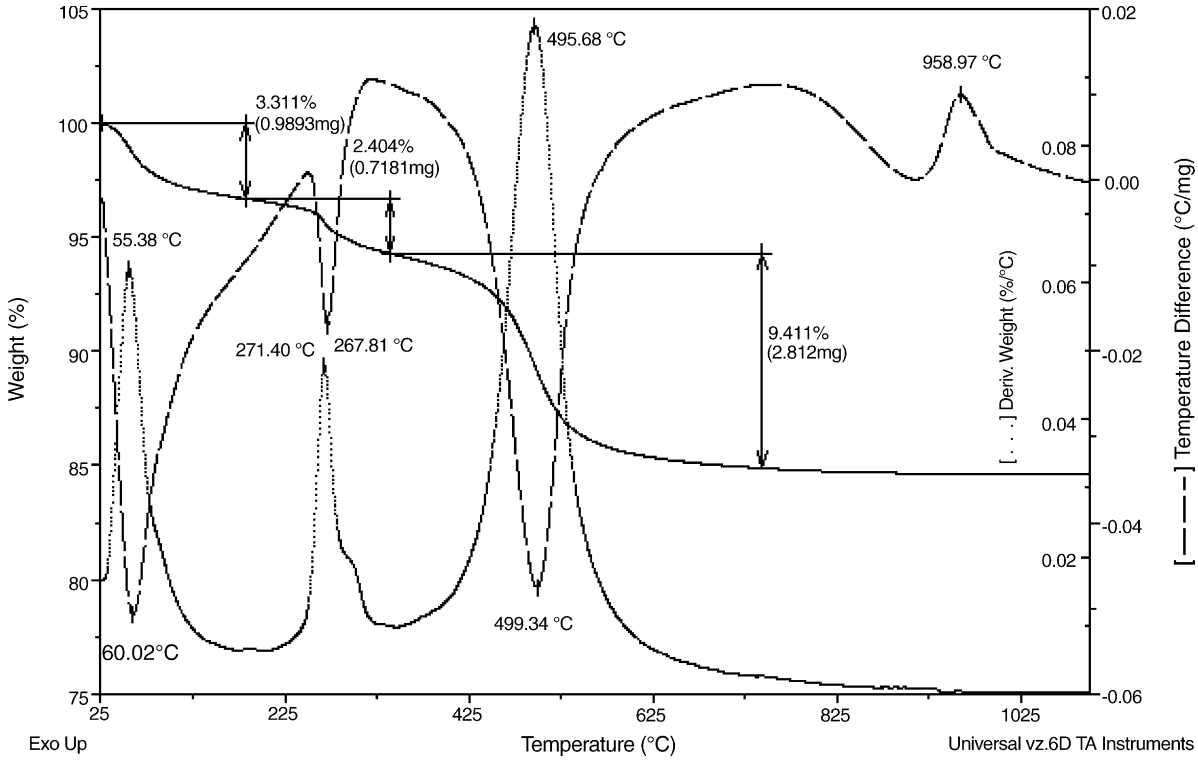

Fig. 3. TG/DTG/DTA curves for the kaolinitic clay.

predomination of distinct sintering mechanisms in these temperature ranges. In the 750–950 °C range there is a small linear shrinkage (1.77–3.82%). In this temperature range solid state sintering, likely by surface diffusion [19], is the dominant sintering mechanism. Necks between contacting platelets grow and smoothening of the particles' surface occurs. The formation of mullite and spinel can also cause densification hence poreless phases substitute porous metakaolinite. In the temperature range above 950 °C, the linear shrinkage ranges from 4.31% to 12.66%. Fig. 5(c and d) shows the pronounced surface smoothening and pore elimination. In this temperature range illite/mica decomposes. The densification behaviour of the red clay is influenced by the sources of flux materials such as K_2O, Na_2O and Fe_2O_3, which favor the formation of a glassy viscous phase. This phase likely begins to form around 960 °C (Fig. 3). Despite the low amount of alkaline fluxes, the viscous phase can be formed at the mentioned temperature range and in a volume enough to cause densification due to the high concentration of iron oxide [20]. The glassy viscous phase infiltrates the pores of the structure and causes densification by liquid phase sintering. The densification mechanism is viscous flow. This mechanism is more effective for densification than solid state diffusion. Three parameters are important to determine the densification rate by the glassy phase formed: the volume of the glassy phase, its viscosity and the wettability of this phase on the solid fraction of the structure. Viscosity and volume are influenced by temperature. The formation of the glassy phase is not a fusion but a diffusion dependent

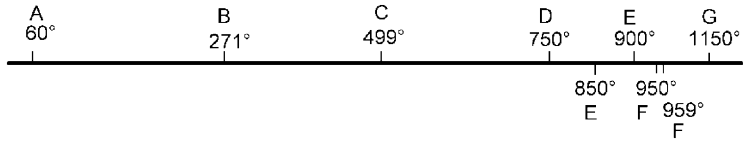

A: Desorption of water from kaolinite
B: Dehydration of gibbsite. Water evolution. $Al_2O_3.3H_2O$ transition alumina
C: Dehydroxylation of kaolinite. $Al_2O_3.2SiO_2.2H_2O \rightarrow Al_2O_3.2SiO_2 + 2H_2O$
D: Gibbsite and kaolinite peaks are not seen. Illite/mica is detected.
E: Peaks of δ-Al_2O_3 are identified.
F: Peaks of γ -Al_2O_3, spinel and mullite are identified. Above this temperature illite/mica. is not detected. Exothermic reaction. Formation of spinel or mullite.
G: Peaks of spinel and mullite are seen.

Fig. 4. Events occurring during sintering of kaolinitic clay with corresponding reaction and temperature range.

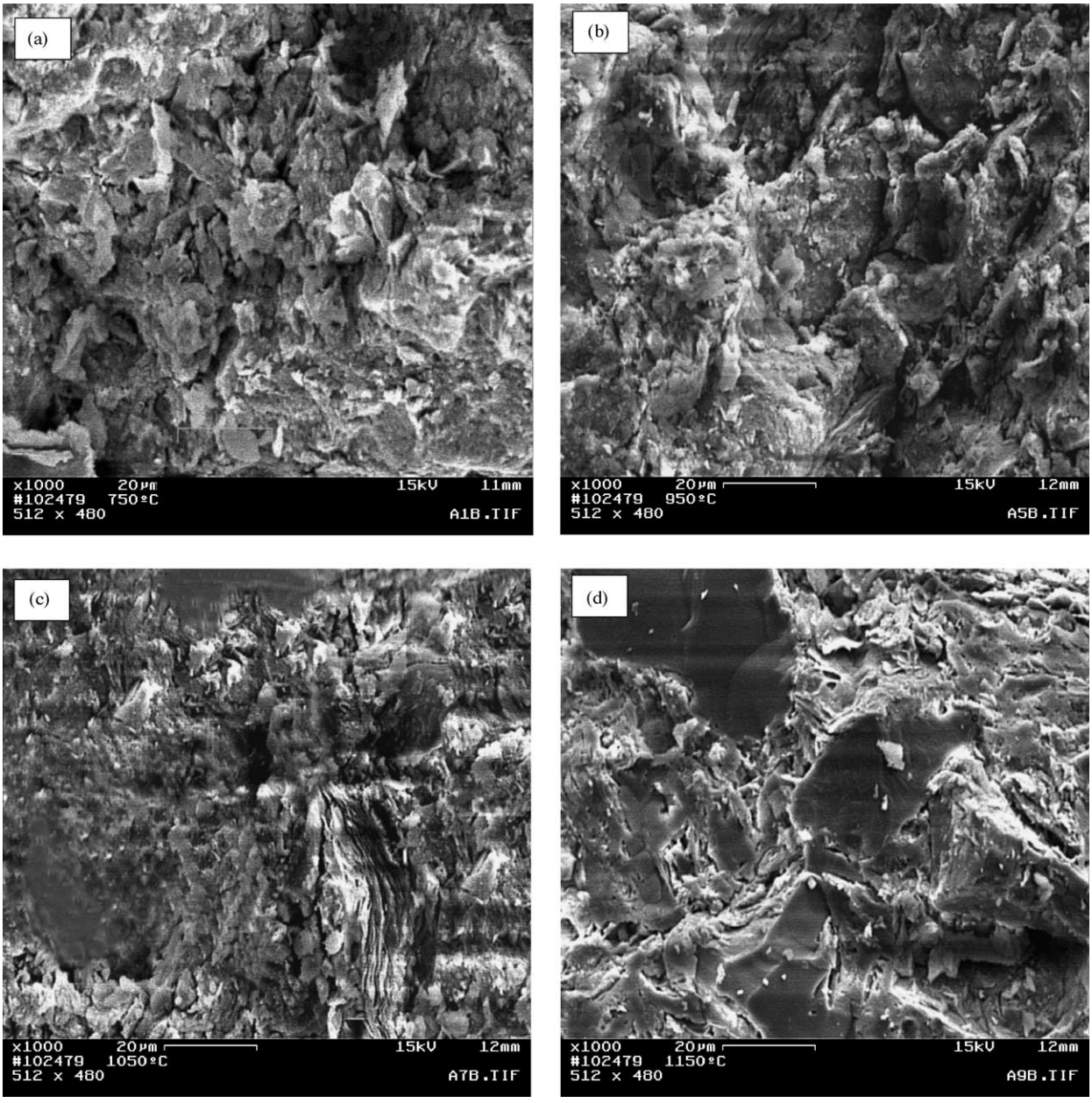

Fig. 5. SEM micrographs of the specimens sintered: (a) 750 °C; (b) 950 °C; (c) 1050 °C; and (d) 1150 °C.

reaction that takes place over a temperature interval. The higher the temperature the lower the viscosity and larger the volume of the glassy phase. Therefore, it is to be expected that densification increases with the temperature increase.

The apparent density and the water absorption are shown in Fig. 8. Density presents only a small variation (1.52–1.57 g/cm^3) in the first temperature range. This occurred due to the combined inverse effects of sintering and weight loss. While the volumetric shrinkage is around three times 3.82%, the weight loss totals near 15%. This results in a small densification, as measured. In the second temperature interval, there is only the effect of sintering and the shrinkage in this interval is rather more intense than in the first range. The apparent density in this intervals varies between 1.61% and 2.08%. The water absorption is related to the volume of the open pores, that is, the pores that are connected with the specimen's surface. The water absorption is closely related to densification. As sintering evolves the pores become rounded and smaller in the solid state sintering range and during the liquid phase sintering range, the pores are isolated from the outer surface and finally closed. Sintering accelerates above 950 °C as the glassy phase is formed. This phase penetrates the pores, closing them and isolating neighboring pores. This explains the intense decrease of the water absorption in this temperature range.

Water absorption (wa) is a parameter that, according to the Brazilian specifications [21], defines the class to which

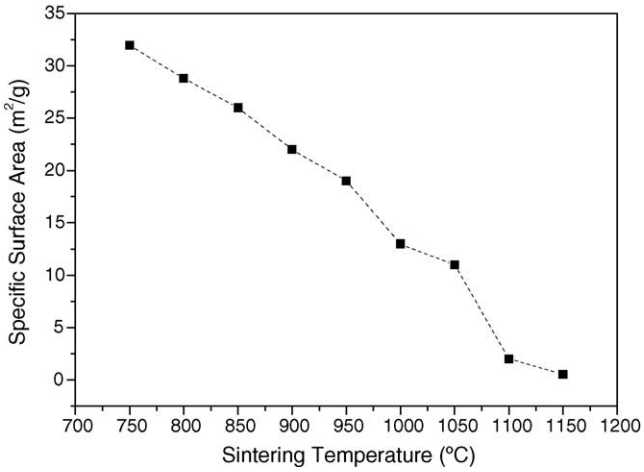

Fig. 6. Specific surface area of the specimens as a function of sintering temperature.

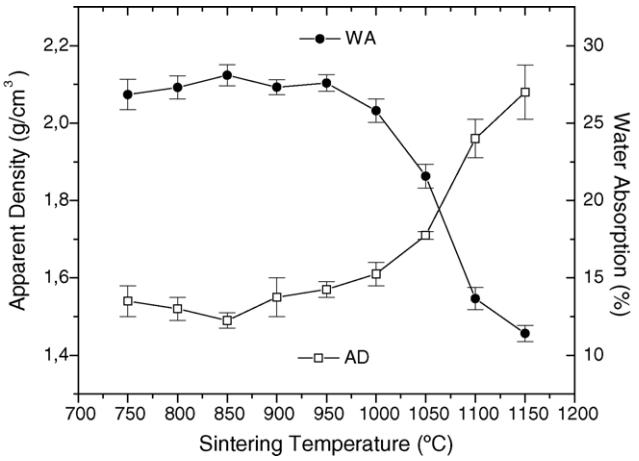

Fig. 8. Apparent density and the water absorption of the specimens as a function of sintering temperature.

any clay-based products suit. In this work we use the following acceptable values to water absorption: bricks (wa $< 25\%$) and roofing tiles (wa $< 20\%$). As shown in Fig. 8 the specimens presented acceptable values for bricks only above 1000 °C. While the specification for roofing tiles is attained only above 1050 °C. These results are very important because explain the low quality of the ceramic products industrially manufactured in Campos-RJ region. The ceramic plants, in general, burn their products in a firing temperature below 950 °C. The characteristics of the red clay from Campos-RJ are responsible by the elevated values of water absorption. The following characteristics can be highlighted: high amount of kaolinite clay mineral, high loss on ignition, low amount of SiO_2, and the presence of hydroxides. In addition, this clay has only a small amount of illitic minerals and alkaline fluxes. These characteristics, therefore, confer the studied red clay a refractory behaviour which impairs sintering during the firing process.

The mechanical strength of the specimens was examined in terms of compressive strength (Fig. 9). The mechanical

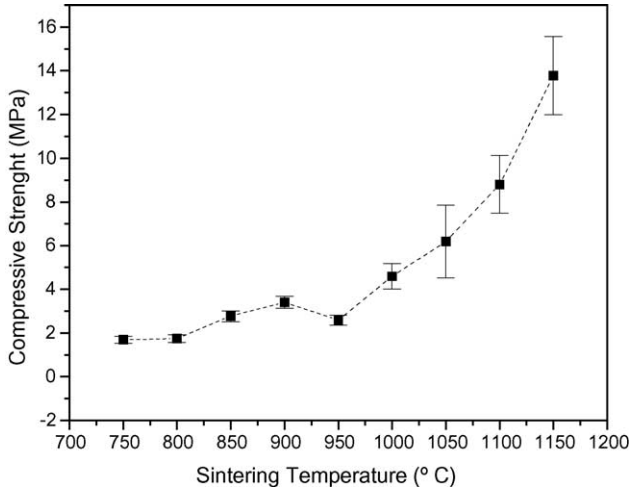

Fig. 9. Compressive strength of the specimens as a function of sintering temperature.

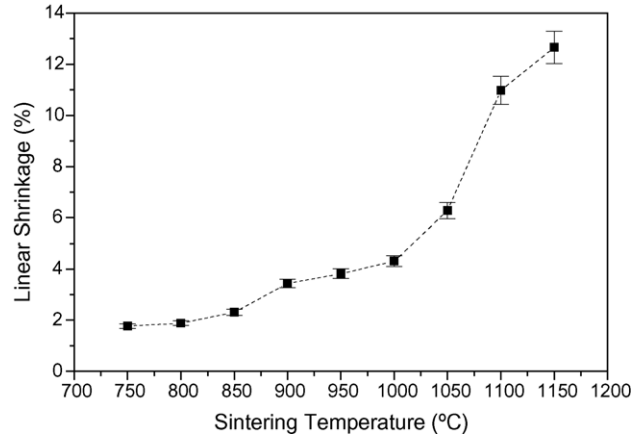

Fig. 7. Linear shrinkage of the specimens as a function of sintering temperature.

behaviour is quite correlated to all the other studied parameters. The compressive strength increases from 4.72 to 17.36 MPa as the sample becomes denser. It is known that porosity influences negatively strength. Therefore, the pore closure must cause an increase of the compressive strength. This is particularly observed above 1000 °C, as the densification rate is high.

4. Conclusions

From the results presented above the following conclusions can be drawn. During firing up to 1150 °C, the red kaolinitic clay bodies undergo a complex series of physical and chemical reactions, involving: hydroxide dehydration, dehydroxylation of clay minerals, phase transformations and partial melting with formation of glassy viscous phase.

These processes play an important role in the densification of the sintered specimens. Two characteristics regions of sintering were observed. The region above 950 °C, with predominance of viscous flow sintering mechanism, caused important changes in the physical–mechanical properties of the specimens.

Water absorption data showed that the brick's specification was achieved only above 1000 °C, while roofing tiles only above 1050 °C. These temperatures are considered as being high relatively in the Campos-RJ region. The Water absorption data also revealed the refractory behaviour of the red clay during firing, which support the difficulty to achieve the desirable level of open porosity by firing at the temperature range used by the local industry (<950 °C). This behaviour is caused by the high amount of kaolinite and low amount of alkaline fluxes in the clays from Campos-RJ. The deficiency of alkaline fluxes is partially compensated by the high amount of iron oxide.

Acknowledgements

The authors would like to thank FAPERJ (process: E-26/171.510/2000) and CNPq (process: 551478/2002-0) for the partial financial support of this work. We would like to thank Dr. Paulo Nagipe for specific surface measurements.

References

[1] P.S. Santos Ciência e Tecnologia de Argilas, second edition, Edgard Blücher, São Paulo, Brazil, 1992.
[2] R.W. Grishaw, Physics and Chemistry of Clays, fourth edition, Ernest Been, London, 1971.
[3] J. Alexandre, F. Saboya, B.C. Marques, M.L.P. Ribeiro, C. Salles, M.G. Silva, M.S. Sthel, L.T. Auler, H. Vargas, Analyst 124 (1999) 1209–1214.
[4] C.M.F. Vieira, J.N.F. Holanda, D.G. Pinatti, Characterization of red ceramic body used in the production of bricks in the region of Campos dos Goytacazes-RJ, Cerâmica 46 (297) (2000) 15–18.
[5] JCPDS-ICCD (1995).
[6] T. Fett, T-stress in rectangular plates and circular disks, Eng. Fract. Mech. 60 (5-6) (1998) 631–652.
[7] F. Chen, Z. Sun, J. Xu, Mode I fracture analysis of the double edge cracked Brazilian disk using a weight function method, Int. J. Rock Mech. Mining Sci. 38 (2001) 475–479.
[8] R.S.T. Manhães, L.T. Auler, M.S. Sthel, J. Alexandre, M.S.O. Massunaga, J.G. Carrió, D.R. Santos, E.C. Silva, A. Garcia-Quiroz, H. Vargas, Soil characterization using X-ray diffraction, photoacoustic spectroscopy and electron paramagnetic resonance, Appl. Clay Sci. 21 (2002) 303–311.
[9] C.F. Gomes, Argilas-O que são e para que servem, Fundação Calouste Gulbenkian, Lisbon, Portugal, 1988.
[10] G.W. Brindley, M. Nakahira, Kinetics of dehydroxylation of kaolinite and halloysite, J. Am. Ceram. Soc. 40 (1957) 346–350.
[11] G.W. Brindley, M. Nakahira, The kaolinite-mullite reaction series: I. A survey of outstanding problems, J. Am. Ceram. Soc. 42 (1959) 311–314.
[12] G.W. Brindley, M. Nakahira, The kaolinite–mullite reaction series: II. Metakaolin, J. Am. Ceram. Soc. 42 (1959) 314–318.
[13] G.W. Brindley, M. Nakahira, The kaolinite–mullite reaction series: III. High-temperature phases, J. Am. Ceram. Soc. 42 (1959) 319–323.
[14] J.W. Halloran, Calcination, Engineered Materials Handbook—Ceramics and Glass, vol. 4, ASM International, USA, 1991.
[15] K. Traoré, T.S. Kabré, P. Blanchart, Gehlenite and anorthite crystallisation from kaolinite and calcite mix, Ceram. Int. 29 (2003) 377–383.
[16] G.W. Brindley, Thermal reactions of clays and clay minerals, Cerâmica 24 (102) (1978) 217–224.
[17] C.J. Mcconville, W.E. Lee, J.H. Sharp, Microstructural evolution in fired kaolinite, Br. Ceram. Trans. 97 (4) (1998) 162–168.
[18] C.Y. Chen, G.S. Lan, W.H. Tuan, Microstructural evolution of mullite during the sintering of kaolin powder compacts, Ceram. Int. 26 (2000) 715–720.
[19] W.D. Kingery, M. Berg, Study of the initial stages of sintering solids by viscous flow, evaporation-condensation, and self-diffusion, J. Appl. Phys. 26 (10) (1955) 1205–1212.
[20] P. Alizadeh, B. Eftekhary Yekta, A. Gervei, Effect of Fe_2O_3 addition on the sinterability and machinability glass-ceramic in the system $MgO–CaO–SiO_2–P_2O_5$, J. Eur. Ceram. Soc. 24 (13) (2004) 3529–3533.
[21] J.L. Francisco, Anuário Brasileiro de Cerâmica Vermelha, Pólo Produções, Criciúma, Brazil, 2001.